

### 4*f*-related electronic structure of $\gamma$ -Ce metal

Takeshi Watanabe and Akimasa Sakuma

*Department of Applied Physics, Tohoku University, Sendai 980, Japan*

(Received 20 December 1984)

The 4*f*-related valence-band density of states (DOS) of cerium metal is derived theoretically by means of the Green's-function technique with a decoupling procedure. A model Hamiltonian includes the Anderson-type mixing term, and the *f*-level degeneracy and spin-orbit splitting are explicitly taken into account. As a result of numerical calculations it was found that the structure near the Fermi edge of the 4*f*-related DOS is markedly influenced by the spin-orbit splitting if the mixing strength is much smaller than the splitting as well as the thermal energy  $k_B T$ . It was also revealed that there appears a peak at a larger binding energy which is very sensitive to the shape of the conduction-band DOS. It is proposed that the present result should give an explanation for the difference between the valence-band photoemission spectra of  $\gamma$ - and  $\alpha$ -Ce metals.

Recent measurements of ultraviolet photoemission spectroscopy (UPS) and bremsstrahlung isochromat spectroscopy (BIS) data have revealed significant difference in the spectral shape near the Fermi edge between  $\gamma$ -phase and  $\alpha$ -phase cerium metals and compounds. According to Wieliczka *et al.*,<sup>1</sup> although the gross features are similar to those reported in the previous experiment,<sup>2</sup> the near edge peak of their UPS data with much improved resolution shows a distinct shoulder at the edge in  $\gamma$ -phase cerium metal whereas the corresponding peak in  $\alpha$ -phase cerium metal exhibits a sharp cutoff. In BIS studies the spectra are markedly different in two phases. The spectra observed by Wuilloud *et al.*<sup>3</sup> clearly indicates the presence of a sharp peak right above the Fermi edge in the  $\alpha$  phase but no such peak in the  $\gamma$  phase. A similar feature was also observed in BIS spectra of compounds, i.e.,  $\alpha$ -type compounds, CeIr<sub>2</sub> and CeRu<sub>2</sub>, which exhibit a sharp peak near the edge while no peak is observed in the  $\gamma$ -type compound CeAl<sub>3</sub>.<sup>4</sup>

Theoretical attempts to explain the presence of the two peaks in UPS and x-ray photoemission spectroscopy (XPS) data have been carried out by several groups. Liu and Ho considered the Coulomb interaction between the localized 4*f* hole and itinerant *d* electrons and showed that two peaks appear depending on whether the hole is screened or unscreened by conduction electrons.<sup>5</sup> In the model proposed by Gunnarsson and Schönhammer the *f*-*d* mixing is introduced by means of the Anderson Hamiltonian and it was shown for the case of infinite degeneracy of the 4*f* level and zero temperature that there is a broad 4*f*-related peak near the bottom of the conduction band and a sharp one very close to the Fermi edge.<sup>6</sup> However, it is difficult to explain by these models, the new feature observed in UPS and/or BIS data of  $\gamma$ -type Ce metal and compounds.

In the present work in order to derive the 4*f*-related density of states (DOS) at finite temperatures we generalize the decoupling method of the equation of motion for the Green's function originally introduced by Lacroix<sup>7</sup> and further consider the spin-orbit splitting and orbital degeneracy of the 4*f* level. The Hamiltonian includes the

Anderson-type mixing as was used in the work by Gunnarsson and Schönhammer and explicitly distinguishes the 4*f* level with different *J* values. The Hamiltonian is given by

$$H = \sum_{k,\sigma} \epsilon_k c_{k\sigma}^\dagger c_{k\sigma} + \sum_{J,M} E_J X_{JM,JM} + \left[ \sum_{k,\sigma} \sum_{J,M} V_{JM,0}^{k\sigma} X_{JM,0} c_{k\sigma} + \text{H.c.} \right], \quad (1)$$

where  $\epsilon_k$  and  $E_J$  are the energies of the conduction electron and the 4*f* levels with  $J = \frac{5}{2}$  and  $\frac{7}{2}$ , respectively, and  $c_{k\sigma}^\dagger$  ( $c_{k\sigma}$ ) is the creation (annihilation) operator for the conduction electron. The projection operator  $|\alpha\rangle\langle\beta|$  are represented by  $X_{\alpha\beta}$ 's, which satisfy the completeness condition

$$X_{0,0} + \sum_{J,M} X_{JM,JM} = 1. \quad (2)$$

Here,  $X_{0,0}$  indicates the projection  $|^1S_0\rangle\langle^1S_0|$  constructing a vacuum space for the 4*f* state. The third term represents the mixing between the 4*f* and conduction states.

The Green's function for the 4*f* electron  $G_{JM}(\omega)$  is defined by

$$G_{JM}(\omega) = -i \int_0^\infty dt \exp(i\omega t) \langle [X_{0,JM}(t), X_{JM,0}]_+ \rangle, \quad (3)$$

where

$$X_{0,JM}(t) = \exp(iHt) X_{0,JM} \exp(-iHt). \quad (4)$$

The 4*f*-related DOS for each *J* is then expressed by

$$\rho_J(\omega) = -\frac{1}{\pi} \text{Im} \sum_M G_{JM}(\omega). \quad (5)$$

To evaluate the Green's function we assume that the potential  $V_{JM,0}^{k\sigma}$  is spherically symmetric around the Ce ion. Then, decoupling the equation of motion for  $G_{JM}(\omega)$  in the second order with respect to the mixing interaction we can write the Green's function  $G_{JM}(\omega)$  as follows:

$$G_{JM}(\omega) = [A_{JM}(\omega) - C] \left[ \omega - E_J - \sum_{k,\sigma} \frac{|V_{JM,0}^{k\sigma}|^2}{\omega - \epsilon_k} A_{JM}(\omega) - B_{JM}(\omega) \right]^{-1}, \quad (6)$$

where  $A_{JM}(\omega)$ ,  $B_{JM}(\omega)$ , and  $C$  are defined by

$$A_{JM}(\omega) = 1 - \sum_{J',M'} \sum_{k,\sigma} \frac{V_{0,J'M'}^{k\sigma} \langle X_{J'M',0} c_{k\sigma} \rangle}{\omega - \epsilon_k + (E_{J'} - E_J)}, \quad (7)$$

$$B_{JM}(\omega) = \sum_{J',M'} \sum_{k,\sigma} \sum_{k',\sigma'} \frac{V_{0,J'M'}^{k\sigma} V_{J'M',0}^{k'\sigma'}}{\omega - \epsilon_k + (E_{J'} - E_J)} \langle c_{k'\sigma'}^\dagger c_{k\sigma} \rangle, \quad (8)$$

and

$$C = \sum_{J',M'} \langle X_{J'M',J'M'} \rangle, \quad (9)$$

respectively. In summations,  $\sum'$ , the term  $(J',M') = (J,M)$  is excluded. The expectation values appearing in Eqs. (7) and (8) can be expressed by using the Green's function  $G_{JM}(\omega)$  as follows:

$$\langle X_{JM,0} c_{k\sigma} \rangle = -\frac{1}{\pi} \text{Im} \int_{-\infty}^{\infty} d\omega f(\omega) \frac{1}{\omega - \epsilon_k + i\delta} V_{JM,0}^{k\sigma} G_{JM}(\omega), \quad (10)$$

$$\langle c_{k'\sigma'}^\dagger c_{k\sigma} \rangle = -\frac{1}{\pi} \text{Im} \int_{-\infty}^{\infty} d\omega f(\omega) \left[ \frac{1}{\omega - \epsilon_k + i\delta} \delta_{k,k'} + \sum_{J,M} \frac{1}{\omega - \epsilon_{k'} + i\delta} V_{0,JM}^{k'\sigma'}(\omega) G_{JM}(\omega) V_{JM,0}^{k\sigma} \frac{1}{\omega - \epsilon_k + i\delta} \right]. \quad (11)$$

Therefore, Eqs. (6)–(11) form simultaneous integral equations for  $G_{JM}(\omega)$ , from which the 4f-related DOS is derived by Eq. (5). We performed self-consistent numerical calculations to obtain  $\rho_{5/2}$  for given shapes of the conduction-band DOS. In the course of calculations the spin-orbit splitting  $\Delta$  is chosen to be 0.3 eV from spectroscopic data,<sup>8</sup> and also temperature ( $k_B T$ ) is taken to be 0.03 eV so that the calculated DOS can be compared with BIS, UPS, and/or XPS data taken at room temperature.

For simplicity it is assumed that the mixing strength  $V_{JM,0}^{k\sigma}$  is constant and therefore we can write

$$\sum_{k,\sigma} (V_{J'M',0}^{k\sigma})^* V_{JM,0}^{k\sigma} \delta(\omega - \epsilon_k) = W(\omega) \delta_{J,J'} \delta_{M,M'}. \quad (12)$$

Here,  $W(\omega)$  is equal to the product of the conduction-band DOS  $D(\omega)$  and  $|V_{JM,0}^{k\sigma}|^2$ . In order to consider the presence of the  $d$  and  $s$  components of the conduction band we assumed the following DOS ( $\omega$  in eV):

$$D(\omega) = D_0 \{ \xi [1 - (\omega/2)^2]^{1/2} + [1 - (\omega/1.5)^2]^{1/2} \}, \quad (13)$$

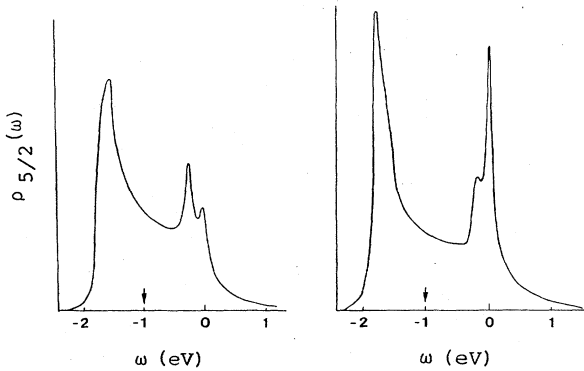


FIG. 1. Calculated 4f-related density of states,  $\rho_{5/2}(\omega)$ , as a function of energy relative to the Fermi edge. The bare 4f level is placed at  $-1$  eV, and  $\bar{W}$  are taken to be 0.0144 eV (left-hand side of the figure) and 0.0196 (right-hand side). The values of  $\Delta$  and  $k_B T$  are 0.3 eV and 0.03 eV, respectively.

which can reproduce approximately the low-energy part of the conduction-band DOS of La metal calculated by Glötzel and Fritsche.<sup>9</sup> Here, the Fermi energy is taken to be 2 eV, as usually assumed, so that the Fermi edge appears at  $\omega=0$ , the center of the two ellipses. The parameters  $D_0$  and  $\xi$  are chosen so as to keep the area of DOS below the Fermi edge equal to  $\pi/2$ . For the sake of convenience to compare with the case of a single semielliptic DOS the two parameters are taken to be  $1 \text{ eV}^{-1}$  and 0.25, respectively. Furthermore, the product  $D_0 |V_{JM,0}^{k\sigma}|^2$  is denoted by  $\bar{W}$ .

In Fig. 1 the 4f-related DOS for the  $J = \frac{5}{2}$  level,  $\rho_{5/2}$ , is shown for two values of  $\bar{W}$ , 0.0144 (left-hand side) and 0.0196 (right-hand side), and the bare 4f level placed at  $E_{5/2} = -1.0$  eV as indicated by the arrow. Also, in Fig. 2 the result for  $E_{5/2} = -0.8$  eV is shown for the same values of  $\bar{W}$ . It is noticed in these figures that the Kondo peak appears slightly above the Fermi edge and its intensity increases with the mixing strength and also as the bare 4f level approaches to the Fermi edge. The characteristic

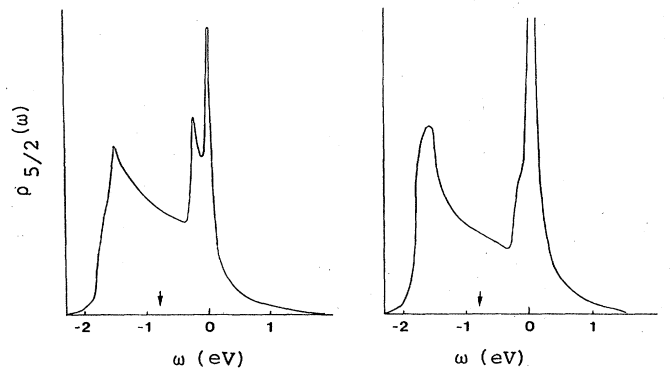


FIG. 2. Calculated 4f-related density of states,  $\rho_{5/2}(\omega)$ , as a function of energy relative to the Fermi edge. The bare 4f level is taken at  $-0.8$  eV, and other parameters are kept the same as in Fig. 1.

feature of the present result is that because of the spin-orbit splitting of the  $4f$  level the Kondo peak observed in  $\rho_{5/2}$  is accompanied by the satellite about 0.3 eV ( $=\Delta$ ) below the main peak. As is shown later the satellite peak appears above the main peak in  $\rho_{7/2}$ . In the case of low mixing as presented by Fig. 1 (left-hand side) the satellite peak is dominant compared with the Kondo peak which is observed almost similar to a shoulder. We believe that the density of states illustrated by this figure corresponds to the case of  $\gamma$ -phase Ce metal, and the peak and shoulder observed in UPS data<sup>1</sup> should reflect the satellite and Kondo peak in a low mixing case. Also, no distinct peak is expected to appear at the Fermi edge in BIS data. As the mixing strength increases as in Fig. 1 (right-hand side) or the bare  $4f$  level approaches to the Fermi edge as in Fig. 2 (left-hand side) the Kondo peak contributes to  $\rho_{5/2}$  as much as the satellite peak, and in a high mixing case the near edge structure of  $\rho_{5/2}$  is predominantly determined by the contribution of the Kondo peak as shown in Fig. 2 (right-hand side), which should give rise to a sharp peak at the Fermi edge both in UPS and in BIS. However, the accuracy of the present approximation is not clear particularly in the case of high mixing for which the result of Gunnarsson and Schönhammer is probably more appropriate, and no quantitative arguments should be made. We are now in the process of developing a different procedure in which the resolvent operator is expanded in the perturbation series.<sup>10</sup>

Finally, in order to investigate how the shape of  $D(\omega)$  of the conduction band affects the  $4f$ -related DOS we carried out numerical calculations for  $D(\omega)$  given by a single semielliptic shape with a full width of 4 eV; i.e.,

$$D(\omega) = D_0 [1 - (\omega/2)^2]^{1/2}. \quad (14)$$

Again the area below the Fermi edge ( $\omega=0$ ) is set equal to  $\pi/2$ , and thus  $D_0$  proves to be  $1 \text{ eV}^{-1}$ . In Fig. 3 both  $\rho_{5/2}$  and  $\rho_{7/2}$  calculated for  $\bar{W}=0.016$  (left-hand side) and 0.02 (right-hand side) are shown. The  $4f$  level is placed at  $-1 \text{ eV}$  as in Fig. 1. It is clear that the peak at a higher binding energy is markedly influenced by the shape of the conduction-band DOS whereas the near edge structure exhibits the feature similar to Fig. 1. If we estimate the Kondo temperature by<sup>11</sup>

$$T_K \simeq \left[ 1 + \frac{D}{\Delta} \right]^{(7/2)/(5/2)} D \exp[E_{5/2}/(5/2)W], \quad (15)$$

it turns out to be 10 K for Fig. 3 (left-hand side) and about 60K for Fig. 3 (right-hand side). Here ( $J$ ) indicates the degeneracy of  $J$  levels and  $D$  is the bandwidth. In Fig. 3 (left-hand side) the spectral weight is dominated by

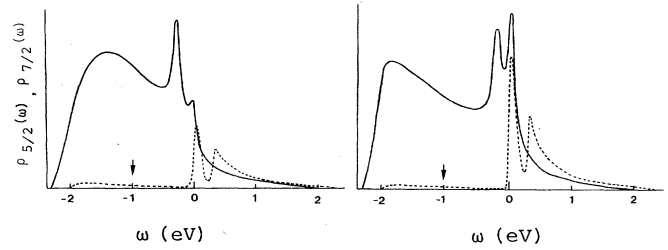


FIG. 3. Calculated  $4f$ -related density of states,  $\rho_{5/2}(\omega)$  in a solid curve and  $\rho_{7/2}(\omega)$  in a dashed curve. The bare  $4f$  level is at  $-1 \text{ eV}$ , and the values of  $\Delta$  and  $k_B T$  are the same as the previous ones. However, the conduction-band DOS  $D(\omega)$  is given by a single semielliptic shape, and  $\bar{W}$ 's are taken to be 0.016 (left-hand side) and 0.02 (right-hand side), respectively. Notice the marked change in the spectral shape of the structure at a lower energy peak.

$\rho_{5/2}$  below the Fermi edge because the spin-orbit splitting is much larger than the Kondo temperature as well as the thermal energy  $k_B T$ . As was mentioned earlier, the Kondo peak observed right above the Fermi edge in  $\rho_{7/2}$  is accompanied by the satellite peak which sits about 0.3 eV above the main peak in contrast to the case of  $\rho_{5/2}$ . This is simply because the  $J = \frac{7}{2}$  level is located above the  $\frac{5}{2}$  level by 0.3 eV and the system gains this amount of energy by transferring an electron from the  $J = \frac{7}{2}$  level to the  $J = \frac{5}{2}$  level in the final state.

In conclusion, we calculated numerically the  $4f$ -related DOS curve at finite temperature considering explicitly the spin-orbit splitting and orbital degeneracy of the  $4f$  level. We believe that the present result obtained for a low mixing case ( $T_K \ll T$ ) should give an explanation to the structure observed in UPS and BIS data of  $\gamma$ -Ce metal and  $\gamma$ -type Ce compounds. In the high mixing case the Kondo temperature estimated from Eq. (15) is almost as much as  $k_B T$  and the approximation used may not be appropriate. We will report on a more general procedure for this case in a separate paper. It should be mentioned that the structure observed at a higher binding energy is very sensitive to the shape of the conduction-band DOS, and therefore the characteristic feature of the conduction-band DOS at least at the lower energy region should be considered when the spectral shape of the peak at a higher binding energy is to be discussed.

The authors acknowledge useful discussions and comments made by C. Horie and Y. Kuramoto. They thank H. Miyazaki for his critical reading of the manuscript.

<sup>1</sup>D. M. Wieliczka, C. G. Olson, and D. W. Lynch, Phys. Rev. B 29, 3028 (1984).

<sup>2</sup>D. M. Wieliczka, J. H. Weaver, D. W. Lynch, and C. G. Olson, Phys. Rev. B 26, 7055 (1982).

<sup>3</sup>E. Wuilloud, H. R. Moser, W.-D. Schneider, and Y. Baer, Phys. Rev. B 28, 7354 (1983).

<sup>4</sup>J. W. Allen, S.-J. Oh, M. B. Maple, and M. S. Torikachvili, Phys. Rev. B 28, 5347 (1983).

<sup>5</sup>S. H. Liu and K.-M. Ho, Phys. Rev. B 26, 7052 (1982).

<sup>6</sup>O. Gunnarsson and K. Schönhammer, Phys. Rev. Lett. 50, 604 (1983); Phys. Rev. B 28, 4315 (1983).

<sup>7</sup>C. Lacroix, J. Phys. F 11, 2389 (1981).

<sup>8</sup>J. Suger, Phys. Rev. B **5**, 1785 (1972).

<sup>9</sup>D. Glötzel and L. Fritsche, Phys. Status Solidi **79**, 85 (1977).

<sup>10</sup>Y. Kuramoto, Z. Phys. B **53**, 37 (1983).

<sup>11</sup>O. Gunnarsson and K. Schönhammer, Phys. Rev. B **28**, 4315

(1983): In this paper the value of  $\delta$  defined by Eq. (A3) is equivalent to the Kondo temperature, and here we assumed that the spin-orbit splitting is much larger than  $\delta$ .